




Cite this: *Chem. Commun.*, 2022, 58, 13059

# Nanometer-scale patterning of hard and soft interfaces: from photolithography to molecular-scale design

Anamika Singh,<sup>a</sup> Anni Shi<sup>a</sup> and Shelley A. Claridge \*<sup>b</sup>

Many areas of modern materials chemistry, from nanoscale electronics to regenerative medicine, require design of precisely-controlled chemical environments at near-molecular scales. Most work on high-resolution interface patterning to date has focused on hard surfaces, such as those for electronics. However, design of interfaces for biological environments increasingly requires precise control over interfaces of soft materials, which is in many cases complicated by nano-to-microscale heterogeneity in the substrate material. In this Feature Article, we describe historical approaches to nanoscale patterning on hard surfaces, challenges in extension to soft interfaces, and an approach to molecular-scale hard and soft interface design based on self-assembled molecular networks, which can be assembled noncovalently on hard surfaces to generate nanometer-scale patterns, then covalently transferred to soft materials including PDMS and hydrogels.

Received 22nd September 2022,  
 Accepted 31st October 2022

DOI: 10.1039/d2cc05221k

[rsc.li/chemcomm](http://rsc.li/chemcomm)

## Introduction

Hierarchical chemical patterning of materials at scales ranging from the molecular scale to the macroscale is important for a wide range of materials, from fabrication of integrated circuits<sup>1</sup> to cell-instructive surfaces for biomedical applications.<sup>2</sup> Despite unprecedented success of lithographic techniques in the mass production of semiconductors, electronics and

integrated circuits, their use in high-resolution patterning of soft materials, such as those for biomedical applications, has been more limited. This is in part due to the high cost and complexity of operation, as well as the incompatibility of soft polymeric materials with harsh processing steps including high-intensity UV irradiation and the use of etchants. The heterogenous structures of many soft materials, which may include pores with diameters from <10 nm to >1000 nm,<sup>3–5</sup> also contributes to challenges in chemical patterning. Overall, inexpensive, scalable methods for nanometer-resolution patterning of soft materials remain a significant challenge.

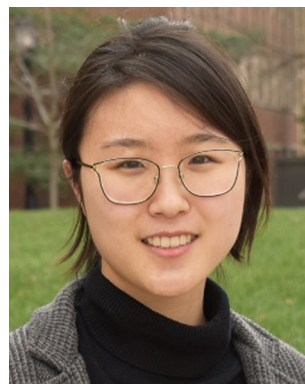
<sup>a</sup> Purdue University, Chemistry, West Lafayette, Indiana, USA

<sup>b</sup> Purdue University, Chemistry and Biomedical Engineering, 560 Oval Drive, West Lafayette, Indiana, USA. E-mail: [claridge@purdue.edu](mailto:claridge@purdue.edu)



**Anamika Singh**

*Anamika Singh graduated from National Institute of Science Education and Research (NISER), India with a BS-MS degree in 2018. At NISER, she worked in the field of asymmetric catalysis, focused on enantioselective hydroboration of prochiral compounds with quaternary carbon centers. In the Claridge group, Anamika is synthesizing amphiphiles with carbohydrate head groups and incorporating such amphiphiles to create nanoscale patterns on 2D surfaces.*



**Anni Shi**

*Anni Shi graduated as an honor student with a BS in chemistry from Wuhan University, China in 2017. Her undergraduate research focused on the design of upconversion nanoparticle-based bioprobes in the bioanalytical laboratory of Prof. Zhihong Liu. In the Claridge group, Anni studied the reaction kinetics of different polydiacetylene amphiphiles, developing a multi-scale view of the reactions of striped phases, as well as assembly at such interfaces.*



Here, we briefly outline several of the commonly used methods for patterning of hard and soft surfaces to provide a broad context for existing capabilities in nanoscale surface patterning, contrasting typical feature resolutions achieved on hard and soft materials. In-depth discussions of specific techniques can be found in other previous reviews.<sup>1,6–11</sup> We then describe surface patterning strategies based on noncovalent molecular network assembly on hard 2D materials, which can be used to produce nanometer-resolution chemical patterns, with a particular focus on striped phases of photopolymerizable functional alkanes. Recently, we have observed that chemical patterns embedded in these molecular layers can be transferred to the surfaces of soft materials including PDMS and hydrogels,<sup>12,13</sup> so we additionally discuss the outcomes of transferring high-resolution functionality to pattern amorphous materials below the length scale of their structural heterogeneity, and applications of this approach.

### Lithographic patterning of hard surfaces at sub-100 nm scales

Surface patterning, frequently referred to as lithography, is often performed using patterns generated by light or beams of charged particles, but can also be achieved using block copolymers, through localized deposition of a molecular ink, or in some cases through mechanical manipulation of the surface (e.g. by rastering a nanometer-scale probe across the substrate).

**Photolithography.** Photolithography, arguably the most common surface patterning technique, uses light and a photo-mask to pattern a photosensitive resist layer, typically on inorganic substrates such as Si, Ga or As.<sup>14</sup> Resolution is limited by the wavelength of light, which led to early restrictions in features that could be achieved using standard optics suited for the visible wavelength range (400–800 nm). Over time, development of short-wavelength optics and other technologies have meant that smaller features can be generated<sup>15</sup>

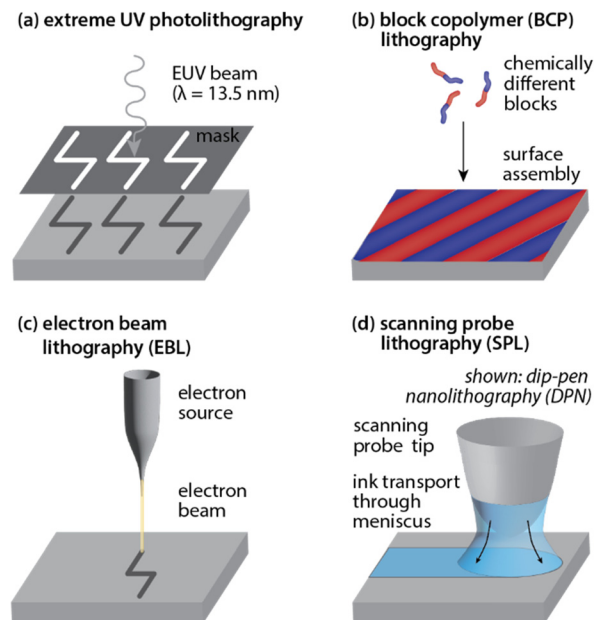


Fig. 1 Overview of a selection of high-resolution interface patterning methods: (a) extreme UV photolithography, (b) block copolymer lithography, (c) electron-beam lithography, and (d) scanning probe lithography.

[e.g. extreme ultraviolet (EUV),  $\lambda = 13.5$  nm, Fig. 1a],<sup>16,17</sup> potentially in combination with other resolution enhancing techniques (off-axis illumination,<sup>18</sup> phase-shifting masking,<sup>19</sup> immersion lithography).<sup>1,6</sup> Such processes are commercially viable;<sup>17</sup> semiconductor fabrication facilities integrate 13 nm resolution features into circuits using EUV lithography. However, fabrication facilities associated with EUV photolithography are extremely expensive; thus, other techniques which can provide similar resolution at much lower cost, albeit with other constraints (e.g. lower throughput, less arbitrary pattern geometry) have emerged in parallel.

**Electron-beam lithography (EBL) and focused ion beam lithography (FIB).** Some lithographic processes take advantage of a beam of high-energy electrons or ions (electron-beam writing,<sup>20,21</sup> ion-beam lithography<sup>7</sup>), which can be focused to produce extremely small spot sizes, to generate nanometer-scale surface features through spatially localized reactions. For instance, electron beam lithography (EBL) uses beam of high-energy electrons to generate arbitrary patterns on electron-sensitive resists (e.g., polymethylmethacrylate (PMMA)) with sub-10 nm resolution.<sup>22</sup> Patterns in the resist can be transferred to the underlying substrate through wet or dry etching, or through lift-off. The resolution of EBL is limited by electron backscattering, which causes scattered electron to interact with unexposed areas. Focused ion beam (FIB) lithography uses heavier ions (e.g. He, Ga, Ne), reducing long-range proximity effects observed in EBL due to the lower backscattering of ions.<sup>23</sup> Most sub-10 nm patterning based on FIB is achieved using He ions, due to sub-nm spot sizes. Costs associated with EBL and FIB are lower than for photolithographic patterning at similar resolution; however serial patterning techniques have much lower throughput than photolithography. For example, it



Shelley A. Claridge

*Graduating with undergraduate degrees in mathematics, biochemistry, and genetics from Texas A&M University, Shelley Claridge worked as a software engineer for six years. She obtained a PhD in chemistry from UC Berkeley in 2008, working with Paul Alivisatos and Jean Fréchet, subsequently working as a postdoctoral fellow at UCLA with Paul Weiss. Claridge joined the Purdue faculty in 2013 and was tenured*

*in 2019; her work at Purdue has been recognized with the NSF CAREER Award, 3M Nontenured Faculty Award, DuPont Young Professor Award, DARPA Young Faculty Award and Director's Fellowship, and Schmidt Science Polymaths Award.*



can take more than 24 hours to pattern 1 cm<sup>2</sup> by EBL.<sup>24</sup> Thus, direct-write systems are primarily used for the fabrication of photomasks for optical lithography and research and development.

**Block copolymer (BCP) lithography.** In comparison to serial techniques, block copolymers (BCPs) provide cost effective, scalable patterning<sup>8,25</sup> which in some cases can produce resolution similar to EBL and EUV,<sup>26–28</sup> albeit with less arbitrary feature geometries (Fig. 1b). BCPs consist of two or more blocks of chemically distinct polymer repeat units; incompatibility between blocks can generate phase separation, producing periodic structures (sphere, cylinder, gyroid, lamellae) with tunable periodicity typically in the range of 5–100 nm.<sup>25,29</sup> In 1997, Adamson *et al.* first demonstrated that BCP nanopatterns can be transferred to silicon nitride with sub-30 nm resolution.<sup>30</sup> However, spontaneous ordering typically generates short range patterns. Ordering has been improved *via* pre-defined physical chemical patterns [directed self-assembly (DSA)],<sup>31</sup> yielding repeating patterns in the range from 5 to 100 nm, depending on polymer block sizes. Introducing new functionalities in BCPs is another way of reducing feature size, and generating utility for a variety of applications.<sup>32</sup>

**Soft lithography.** Soft lithography,<sup>10,33,34</sup> often referred to as microcontact printing ( $\mu$ CP), was introduced by Whitesides and coworkers in 1993. This method enables micro- and in some cases nanoscale geometric patterning of molecular inks to control local surface chemistry. Relatively rapid and inexpensive patterning is achieved by replicating a master Si mold, typically created by photolithography. An elastomeric stamp (*e.g.*, polydimethylsiloxane (PDMS)) is then cast as a negative replica of the Si master. The elastomeric stamp can be inked with desired material to transfer patterns onto a variety of substrates, generally relatively hard surfaces that withstand pressures required for molecular ink transfer.<sup>35</sup> Feature resolution is usually on the order of  $\mu$ m, but can be reduced through the use of specialized transfer conditions. For instance, one significant challenge in regards to pattern resolution is the diffusion of molecular ink around the edge of the stamp pattern; the use of high-molecular-weight inks (*e.g.* 20-carbon alkanethiol,<sup>36</sup> or dendrimeric polymer<sup>37</sup>) has produce features  $\sim$ 80 nm and  $\sim$ 40 nm in size, respectively. Additionally, the ‘printing’ process can be reversed, using an activated PDMS stamp to remove sections of a monolayer, a process referred to as chemical lift-off lithography.<sup>38–40</sup> Through the use of multiple lift-off steps, features  $<$ 50 nm can be achieved.

**Nanoimprint lithography (NIL).** In 1995, Chou and coworkers first used NIL to pattern metals (Au and Ti) on a Si wafer with sub-25 nm resolution.<sup>41</sup> NIL is performed by pressing a rigid mold (typically Si) with a nanoscale pattern into a thermoplastic film (*e.g.*, PMMA) heated above its glass transition temperature (100–200 °C). Subsequent cooling (to 20–80 °C) results in transfer of the mold pattern to the polymer film. Set-and-flash lithography (S-FIL) extends this technique, using UV transparent quartz molds to pattern photo-curable polymer films, avoiding the use of high temperature. NIL resolution is dependent on mold feature size; high resolution molds (sub-10 nm) are typically prepared by EBL (Fig. 1c).

**Scanning probe lithography (SPL), including dip-pen nanolithography (DPN).** Scanning probe lithographic methods<sup>42,43</sup> rely on sharp probes (tip radii usually  $<$ 10 nm) to fabricate nanoscale features (Fig. 1d). One increasingly common SPL approach is DPN,<sup>44</sup> introduced by Mirkin and coworkers in 1999,<sup>45</sup> which was initially used to pattern alkanethiols on gold substrates with sub-50 nm resolution. In general, DPN uses an atomic force microscope (AFM) probe ‘pen’ coated with a molecule- or materials-based ‘ink.’ The ink is deposited onto the substrate *via* diffusion through a meniscus that forms between the tip and substrate under ambient conditions. Although AFM tips often have a radius of curvature  $\sim$ 10 nm, pattern resolution is also determined by the physics and morphology of the meniscus, and potentially (as for  $\mu$ CP) further diffusion of molecular ink at the interface.<sup>46–48</sup> Over time, DPN has evolved to template many types of materials (*e.g.*, polymers, colloidal nanoparticles, sol-gel precursors, biomolecules including proteins and oligonucleotides, and single virus particles and bacteria) on a variety of surfaces (including metals, semiconductors, and insulators). Initially a low-throughput serial technique, DPN throughput has been increased by parallelizing the deposition process,<sup>49</sup> using large arrays of tips (in some cases  $>$ 50 000) for parallel printing.<sup>50</sup> In even more highly parallelized approaches (in some cases  $>$ 10 million tips) softer polymer tips are often utilized to allow for simultaneous contact with hard substrates that exhibit imperfect surface topographies.<sup>51</sup>

#### Patterning of soft surfaces

Several of the methods discussed above have also been used to chemically pattern soft surfaces (*e.g.* hydrogels) including photo-immobilization, inkjet printing, microfluidics, and  $\mu$ CP;<sup>11</sup> in some cases, physical patterning (*e.g.* based on wrinkling instabilities) is also possible.<sup>52,53</sup> While techniques such as inkjet printing that operate in the 20–50  $\mu$ m size regime can produce similar feature sizes for both hard and soft surfaces, for high-resolution techniques, typical feature sizes on soft substrates are substantially larger than for the same technique applied on flat crystalline surfaces. In part, this is due to topographical and chemical heterogeneity of the substrate. Many soft materials based on polymers (*e.g.* PDMS, hydrogels) have pores, which may range in size from less than 10 nm to greater than 1000 nm, depending on the material. Thus, patterning below the length scale of heterogeneity in the material is often challenging.

**Electron-beam lithography.** For instance, EBL has been used to pattern soft materials<sup>54</sup> including polyethylene glycol (PEG)<sup>55</sup> and poly(*N*-isopropylacrylamide) (PNIPAM),<sup>56</sup> typically by using the electron beam to induce local cross-linking of the polymer in a dry, spin-coated film; subsequent swelling of the patterned polymeric material can display patterned functional groups for interactions with biomolecules (Fig. 2a). While EBL routinely generates 1 nm feature sizes on hard materials, typical minimum reported linewidths for soft material patterning are on the order of 100 nm.

**Photolithography.** Photochemistry is commonly utilized in the curing of hydrogels, and one- and two-photon photopatterning have been used to localize crosslinking of small molecules and





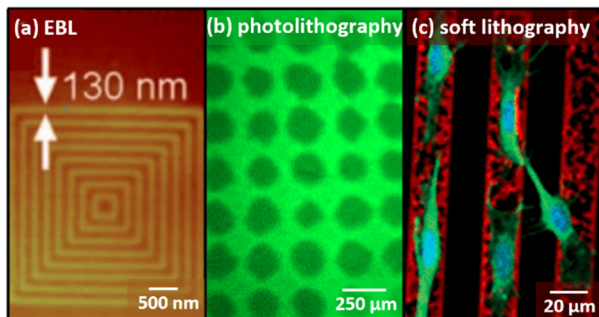


Fig. 2 Typical feature sizes on soft substrates (a) nanoscale patterns of maleimide-PEG and biotin-PEG. (b) ACRL-PEG-RGDS patterns on PEGDA hydrogels (c) fibronectin (20  $\mu\text{m}$  in width) patterned on gelatin hydrogels. Adapted from ref. 54, 57, and 35, with permission. Copyright 2009 American Chemical Society, 2006 Elsevier, and 2011 Royal Society of Chemistry, respectively.

biomolecules in and on the hydrogel (Fig. 2b).<sup>57–60</sup> Early examples of this approach by West and others used PEG diacrylate (PEGDA) hydrogels as a base material, then applied radiation (from the illumination laser of a confocal microscope, or illumination through a patterned transparency) to additionally crosslink a thin layer of acryloyl-PEG-peptide, producing feature widths  $\sim 5 \mu\text{m}$ . Additional work by Anseth and others has demonstrated photo-initiated thiol-ene click reactions to locally append peptides and other molecules to hydrogels.<sup>61</sup> Later, refinement of the process using multiphoton patterning strategies decreased feature sizes to  $1 \mu\text{m}$   $x$ - $y$ ,  $3$ – $5 \mu\text{m}$   $z$ .<sup>60,62</sup> Typical conditions used for this approach result in  $0.1$ – $1.0$  mM labeling with peptide,<sup>63</sup> corresponding to volumetric densities as high as 1 peptide per  $1600 \text{ nm}^3$  (for 1 mM labeling).

**Soft lithography.**  $\mu\text{CP}$  has also been used to pattern biological molecules on soft surfaces (e.g. PDMS, hydrogels, Fig. 2c). For instance, shaped PDMS stamps inked with fibronectin (FN) or other extracellular matrix (ECM) proteins have been used to pattern flat PDMS,<sup>64,65</sup> typically in islands designed to control adsorption, spreading, and differentiation of individual cells (e.g.  $25 \mu\text{m} \times 25 \mu\text{m}$  or  $50 \mu\text{m} \times 50 \mu\text{m}$ ).<sup>66</sup> However,  $\mu\text{CP}$  of hydrogels is often problematic, in part due to lower Young's modulus and higher surface energies of such materials in comparison with PDMS. Chemical modification of the PDMS stamp or hydrogel surface may be used to promote transfer; for instance, disulfide-linked polyacrylamide gels have been used as substrates for  $\mu\text{CP}$  with biotin derivatives ( $2 \mu\text{m}$  patterned line widths), which were subsequently used to pattern further adsorption of proteins.<sup>67</sup> In some cases, hydrogels can also be lyophilized to stabilize the material for  $\mu\text{CP}$  transfer of molecules. For instance, Castaño and coworkers lyophilized Matrigel and gelatin substrates, and used PDMS to print FN lines with widths  $2$ – $20 \mu\text{m}$  on the lyophilized gels, which were then rehydrated and used to direct growth of NIH-3T3 cells.<sup>35</sup>

### Chemical patterning of hard materials with self-assembled molecular networks: 1 nm features with diverse chemistry

Most broadly utilized molecule-based patterning approaches for hard materials use standing phases of alkanethiols on gold

or glass substrates; however, self-assembled molecular networks (common on 2D materials) represent an underutilized and potentially transformative means to generate useful sub-10 nm chemical patterns on both hard and soft materials. Molecular network assembly on highly oriented pyrolytic graphite (HOPG), and in some cases on other 2D materials (e.g. graphene,  $\text{MoS}_2$ ,  $\text{WS}_2$ , black phosphorus), takes advantage of weaker molecule-substrate interactions and directional molecule-molecule interactions which allow for long-range molecular ordering based on the local flatness of the substrate.<sup>68,69</sup> Together, these aspects of assembly enable diverse chemistries and symmetries to be designed into molecular patterns with 1 nm-resolution features, well below scales that can be easily achieved in conventional standing phase monolayer chemistries on gold. Here, we discuss this chemical patterning strategy, with a focus on patterning using striped phases of polymerizable alkyldiacetylenes, since this strategy has proven extensible to high-resolution patterning of soft surfaces.

High-resolution chemical patterning based on molecular assembly on HOPG has its roots in early experimental observations in the lubrication community, which showed long-chain hydrocarbons have large enthalpies of adsorption on cast iron (containing as little as 1% carbon impurities), as well as on graphite,  $\text{MoS}_2$ , and  $\text{WS}_2$ .<sup>70,71</sup> Models developed by 1970 suggested that, in the case of graphite, this might be in part due to lattice matching between the hexagonal graphite lattice (center-to-center distance  $2.46 \text{ \AA}$ ) and the zig-zag structure of the alkyl backbone ( $2.56 \text{ \AA}$ ).<sup>72</sup> With the development of scanning probe microscopy, Rabe<sup>73</sup> and others<sup>74,75</sup> began to observe that long-chain alkanes not only adsorbed with their chains parallel to the interface, but could form ordered linear patterns (also referred to as lamellar or striped phases) oriented in epitaxy with the HOPG lattice (Fig. 3).

Striped phase assembly of functional alkanes results in ordering of the functional headgroups into 1 nm-resolution

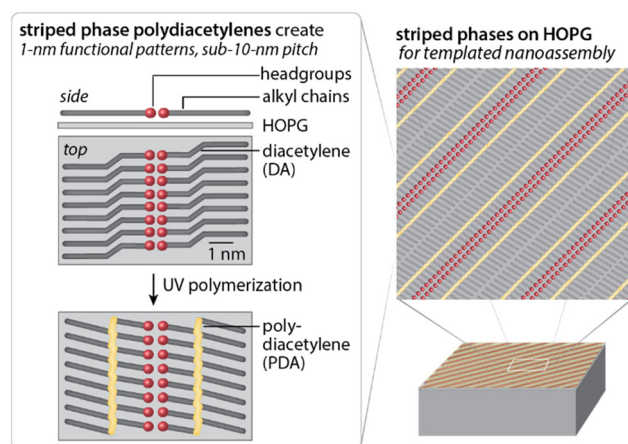


Fig. 3 Schematic of striped-phase assembly on HOPG to generate 1 nm-resolution chemical patterns with sub-10 nm pitch, and PDA polymerization to set the chemical pattern. Adapted from ref. 121 with permission. Copyright 2021 John Wiley and Sons.



patterns with a pitch (*ca.* 5–10 nm) determined by the length of the alkyl chain.<sup>74,75</sup> Many types of functional headgroups can be embedded in such monolayers to act as nanometer-scale patterning elements, and can contribute to molecular ordering and pattern symmetry. For instance, H-bonding headgroups (*e.g.* carboxylic acids, amines, alcohols)<sup>74,75</sup> can induce directional pairing at the lamellar periphery, reorienting alkyl chains relative to the lamellar axis. Conversely, molecules with functional headgroups that are wider than the alkyl backbone can locally alter lateral alkyl chain packing distances, in some cases leading to interdigitated alkyl chain structures that halve the lamellar width.

Pattern symmetry can be modified in a number of ways, including by appending functional moieties and/or alkyl chains to an aromatic core, diversifying the functional patterns that can be installed at the interface.<sup>68,76–80</sup> Directional interactions can be achieved through H-bonding,<sup>81</sup> halogen bonding,<sup>82,83</sup> or dipole–dipole interactions,<sup>84,85</sup> as well as metal coordination. Binary and in some cases higher-order molecular patterns can also be used to establish additional pattern complexity.<sup>81</sup>

Functional patterns established through self-assembled molecular networks are typically non-covalently adsorbed to the substrate. In some cases, pattern stability can be increased using reactions that introduce covalent bonds between pattern elements (*e.g.* polydiacetylene photopolymerization,<sup>86,87</sup> thiophene polymerization,<sup>88</sup> Ullman coupling,<sup>89,90</sup> boronic acid polycondensation<sup>91–94</sup>). For instance, functional alkanes with embedded diacetylene groups can undergo topochemical photopolymerization to generate a conjugated polydiacetylene (PDA) backbone<sup>86</sup> that links molecules over tens to hundreds of nanometers. Attractive aspects of this reaction include the photoactivation, which enables it to be carried out without the introduction of additional solvents or reactions following pattern formation. Additionally, the polymerization reactions have been well-studied in 3D crystals and in Langmuir films,<sup>95–100</sup> with the result that a small range of appropriate monomers are commercially available. Of these, 10,12-diyne acids such as 10,12-pentacosadiynoic acid (PCDA) have been the most broadly studied using scanning tunneling microscopy (STM), by the groups of Okawa and others.<sup>87,101–104</sup> In the context of STM studies, polymerization can be carried out not only with UV irradiation, but also by using tunneling electrons from the STM tip, generating individual conjugated PDAs that have been studied with an interest in molecular electronics.

**Influence of lying-down monolayer structure on chemical properties.** The nm-scale chemical environments generated in such patterned interfaces represent highly unusual surface chemistry, with tightly confined polar environments surrounded by nonpolar environments, somewhat analogous to environments in protein binding pockets. The highly confined dielectric environment is an important contributor to functionality due to the very small scales of polar and nonpolar environments in these layers—for instance, some of the earliest work from our group<sup>105,106</sup> showed that while carboxylic acids in aqueous solution have a  $pK_a \sim 5$ , COOH groups in these monolayers have a  $pK_{1/2}$  of 9–10 (Fig. 4f), due to the limited

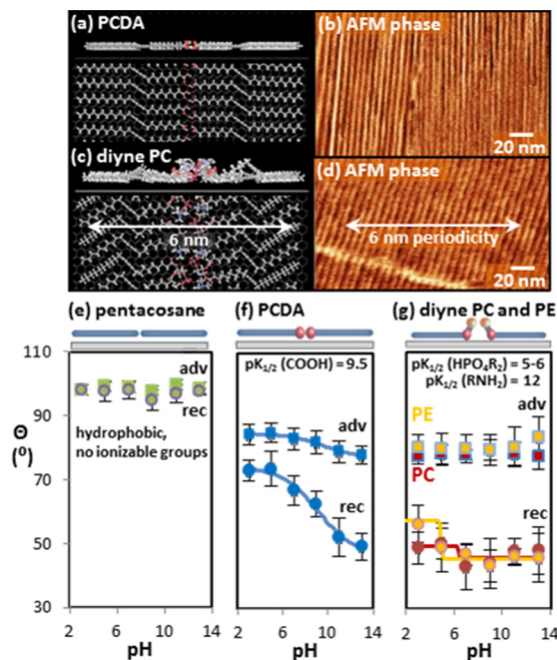


Fig. 4 (a) Molecular model and (b) AFM image of PCDA/HOPG striped phase, and (c) model and (d) AFM image of diyne PC/HOPG striped phase. (e–g) Contact angle titrations for (e) pentacosane, (f) PCDA, and (g) diyne PC and diyne PE. Adapted from ref. 105 with permission. Copyright 2016 American Chemical Society.

ability of the surrounding interface to stabilize the charged form of the COOH group. From a functional perspective, this means that COOH striped phases on HOPG would be expected to be predominantly neutral under physiological conditions. When phosphoethanolamine is assembled into striped phases, the phosphate group undergoes a similar ( $\sim 5$  unit) shift in  $pK_{1/2}$  (Fig. 4g), meaning that it absorbs the chemical impacts of the nonpolar interface. In contrast, the terminal primary amine retains its standard solution ionization behavior. Overall, this suggests that the phospholipid headgroup represents an atom-efficient means to control weak acid and base chemistry in confined 1D dielectric environments at interfaces.<sup>105</sup> Striped phases also impact nanoscale wettability, creating directional wetting effects for ultrathin films of liquid,<sup>107</sup> meaning that chemical effects of the interface extend several nm into the solvent environment.

**Long-range molecular ordering in lying-down monolayers.** Many applications based on chemical patterning of interfaces require control over substrate chemistry not just at the molecular scale, but up to scales of  $\mu\text{m}$ , cm, or even larger. However, most previous work on striped phases aimed at molecular electronics had been carried out with STM as the primary characterization technique, meaning that typical image sizes were  $< 100$  nm edge length. To use the striped phase chemistry for larger-scale applications, our group has developed protocols and devices that extend ordering to  $\mu\text{m}$  and larger scales,<sup>108–110</sup> with some protocols routinely generating ordered molecular domains  $> 100 \mu\text{m}^2$ , relevant to controlling interactions with cells. Long-range molecular ordering is typically achieved





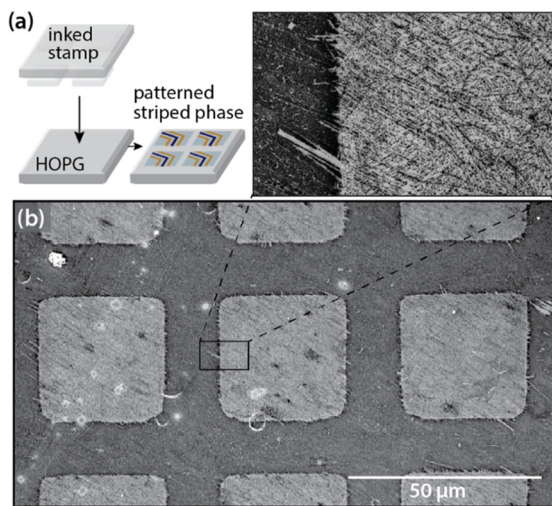


Fig. 5 (a) Schematic of microcontact printing of striped phases on HOPG with geometric control. (b) SEM image of microcontact printed patterns of striped PDAs (sPDAs) on HOPG. Adapted from ref. 113 with permission. Copyright 2020 American Chemical Society.

through a process we term Langmuir–Schaefer (LS) conversion, assembling a standing phase monolayer of amphiphiles on an aqueous subphase, and lowering an HOPG substrate onto the standing phase, allowing for molecular transfer to the 2D material surface. A significant finding in relation to LS conversion was that controlled elevation of the HOPG temperature during transfer greatly enhances molecular ordering.<sup>108</sup> A more recent version of this process incorporates a thermally-controlled rotary transfer stage, prototyping roll-to-roll transfer.<sup>111</sup>

We have also found that it is possible to use microcontact printing ( $\mu$ CP) to generate microscale geometric patterns (*e.g.* squares, Fig. 5) comprised of nm-wide chemical stripes,<sup>112</sup> including amphiphiles with complex headgroup chemistries (*e.g.*, phosphoinositol, a phospholipid that incorporates an inositol carbohydrate in the headgroup). To generate additional chemical complexity, striped patterns of amphiphiles can also act as displaceable templates, controlling assembly of complex molecules (*e.g.*, end-functionalized diphenylalanine (FF) peptides) by controlling access to the aromatic substrate on the scale of the assembling molecule footprint.<sup>113</sup>

**Chemical impacts of nm-resolution chemical templates: directing assembly of gold nanowires (AuNWs).** Patterned interfacial functional groups can also direct assembly of meso-to-microscale objects (*e.g.* inorganic nanowires), leveraging the anisotropy of the chemical template to orient anisotropic nanostructures at the interface (Fig. 6). Previously, studies by Chi, Perepichka, and others had observed that it was possible to use noncovalent molecular template layers to control adsorption of isotropic inorganic clusters (*e.g.* Au55).<sup>114,115</sup>

We observed that striped molecular patterns with strong dipoles in the headgroups (*e.g.* phosphoethanolamine) were capable of orienting and ordering ultranarrow gold nanowires (AuNWs), pointing to the importance of specific chemistries

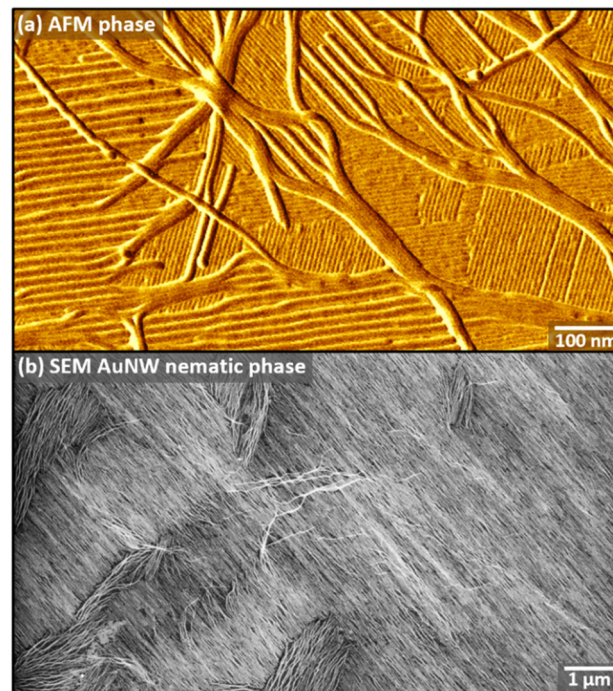


Fig. 6 (a) AFM phase image of AuNWs adsorbed to a phospholipid sPDA with small domains, illustrating differences in wire assembly when misaligned vs. aligned with the sPDA lamellar axis. (b) SEM images of AuNWs assembled on dPE sPDA with long-range order. Adapted from ref. 116 with permission. Copyright 2019 Cell Press.

embedded in these functional patterns.<sup>116</sup> High-resolution AFM images illustrate that when wires are aligned with the striped template, they separate to distances up to 30 nm (Fig. 6a), with highly aligned arrays of AuNWs achieved over areas of many  $\mu\text{m}^2$  (Fig. 6b).<sup>117–119</sup> Overall, these findings point to a potentially broad-impact design principle: polar functional groups common in biology can impact their environment over much greater distances in nonpolar solvents common in synthetic materials.

### Chemical patterning of soft surfaces with lying-down monolayers

Most classical surface science approaches to achieving precise molecular order and functionalization rely on atomic order in the substrate lattice to achieve ordering of molecules that adsorb to the surface. However, many emerging materials applications, particularly those that interface with biology, utilize amorphous soft materials with heterogeneous surfaces. This raises significant challenges in precise control of surfaces for wearable electronics and cell culture, for example, to control ligand clustering for interactions with cells; as mentioned earlier, most patterning methods (*e.g.*, EBL, photolithography) that are useful on hard surfaces provide decreased resolution on soft materials.

Recently, we have found that it is possible to assemble molecular networks with embedded 1 nm-resolution functional patterns on HOPG, polymerize to set the functional pattern,



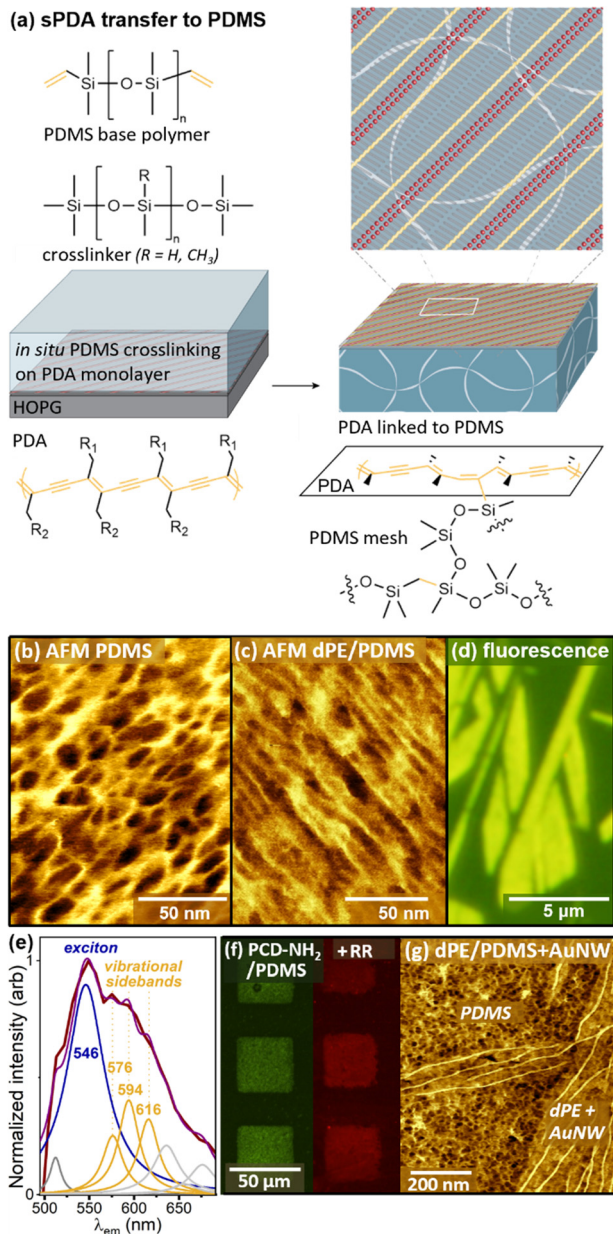


**Fig. 7** (a) Schematic of sPDA transfer from HOPG to PDMS. (b,c) AFM images of (b) unfunctionalized PDMS, and (c) PDMS with transferred dPE sPDA layer. (d) Fluorescence micrograph of dPE transferred to PDMS. (e) Fluorescence emission spectrum of dPE/PDMS. (f) Fluorescence micrographs of PCD-NH<sub>2</sub> sPDAs on PDMS as-transferred (left) and after reaction with derivatized rhodamine red (right). (g) AuNWs adsorb only in sPDA-functionalized regions of PDMS, recapitulating assembly behavior on sPDAs on HOPG. Adapted from ref. 12 with permission. Copyright 2021 American Chemical Society.

then transfer polymerized striped phases from HOPG to other materials (Fig. 7), taking advantage of the sPDA backbone as a scaffold to stabilize the nm-scale chemical patterns during transfer.<sup>12,13</sup> Transfer is achieved using reactions (e.g. hydrosilylation or acrylate radical-mediated polymerization) that form covalent links to the sPDA polymer backbones in the monolayer molecular network.

Transfer of sPDAs to PDMS (Fig. 7a), takes advantage of the PDMS crosslinking reaction, which is carried out *in situ*, with the liquid PDMS reaction mixture in contact with the sPDA. PDMS crosslinking typically involves covalent bond formation between Si-H groups in the PDMS crosslinker and vinyl groups in the PDMS base polymer, in the presence of a transition metal catalyst. When carried out in contact with an sPDA monolayer, crosslinks are also formed with the PDA backbone. After curing, exfoliation of the PDMS from the HOPG also removes sPDAs covalently linked to the PDMS surface. After transfer, the monolayer is visible at small scales in AFM images. Fig. 7b shows unfunctionalized SYLGARD 184 PDMS, with a mesh size of approximately 10 nm. Fig. 7c shows the same PDMS blend cured in contact with dPE/HOPG as shown in Fig. 7a; here, linear features are visible along the PDMS surface. At larger scales, transfer can be characterized based on fluorescence emission from the sPDA backbones (Fig. 7d and e). Following transfer, the monolayer headgroup chemistry can be utilized for post-functionalization or further assembly (e.g. with rhodamine derivatives, Fig. 7f, assembly of AuNWs, Fig. 7g, or controlled adsorption of oppositely-charged electrolytes).<sup>12,120</sup>

Characterizing chemistry at soft, porous interfaces is an ongoing challenge; however, the sPDA transfer approach benefits from the ability to readily extract information regarding nm-scale interface structure on HOPG prior to transfer, and correlate with interface properties on the soft material after transfer.<sup>121,122</sup> For instance, individual polymerization events on HOPG can be characterized by AFM, based on Å-scale topographical protrusion of the sPDA backbone following polymerization. Correlating nanoscale extent of polymerization on HOPG (Fig. 8a, main images) with microscale sPDA transfer (quantified through sPDA fluorescence emission, Fig. 8a, insets) enables a multiscale view of the polymerization process. Already, this approach has allowed us to identify a large and previously unreported difference in polymerization efficiency between the two most common commercially available monomers for striped phases, PCDa (referred to here as PCD-COOH for clear comparison with PCD-NH<sub>2</sub>) and tricosadiynoic acid (TCD-COOH) (Fig. 8b, dotted grey lines), enabling design new high-efficiency monomers for polymerization and surface functionalization of PDMS.

More recently, we have extended this understanding to the transfer of molecules with different headgroup chemistries, such as amines (Fig. 8b, blue and gold lines). The ability to quantify lengths of large populations of individual polymers on HOPG has allowed us to develop models of sPDA transfer to PDMS that relate the degree of polymerization (DP), probability of crosslinking per PDA unit ( $p_{\text{rxn}}$ ), and the number of crosslinks required for sPDA exfoliation ( $n$ ), as illustrated in Fig. 8c. Overall, these models point to the likelihood that at least 2 crosslinks are required for PDA exfoliation, with  $p_{\text{rxn}}$  in the range of 1–3% per PDA unit (Fig. 8e).

While PDMS is broadly used for many applications including microfluidics, other classes of more hydrophilic polymers (e.g. hydrogels) are more commonly used in applications that require direct contact with biological environments. We have





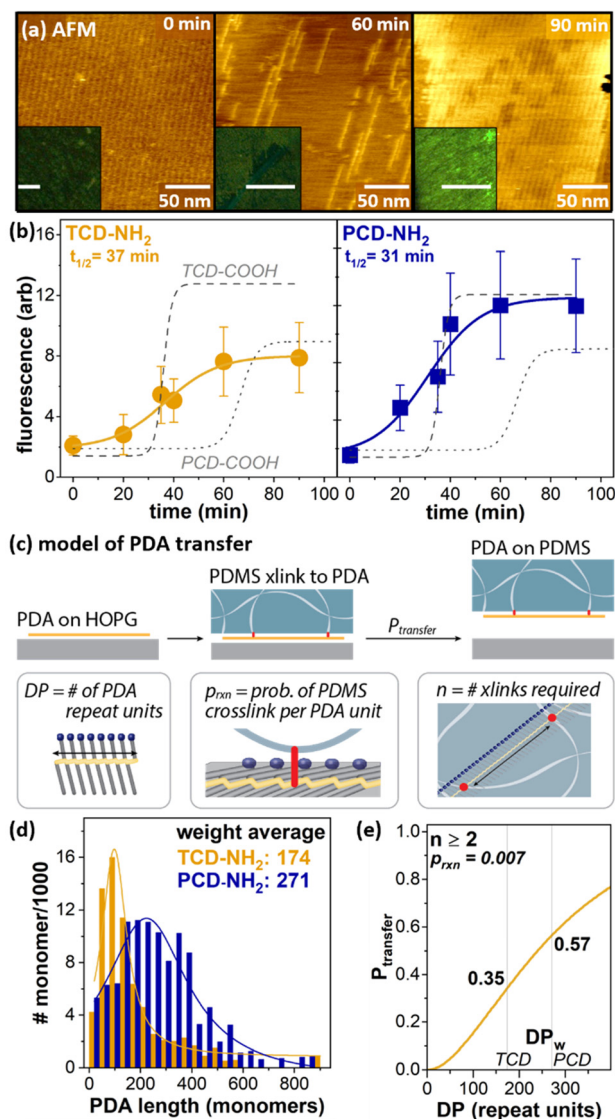


**Fig. 8** (a) AFM and fluorescence characterization of PCD-COOH polymerization at 0 min, 60 min, and 90 min, illustrating that fluorescence intensity of material transferred to PDMS increases with the extent of polymerization on HOPG. (b) Fluorescence of TCD-NH<sub>2</sub> (left) and PCD-NH<sub>2</sub> (right) transferred to PDMS after different periods of UV polymerization on HOPG. Dotted lines illustrate comparison with structurally analogous carboxylic acids. (c) Probabilistic model describing sPDA transfer to PDMS. (d) Histogram of weight average degree of polymerization for TCD-NH<sub>2</sub> and PCD-NH<sub>2</sub> on HOPG. (e) Calculated fractional transfer for TCD-NH<sub>2</sub> and PCD-NH<sub>2</sub>, based on model and on experimentally observed populations of polymer lengths. Adapted from ref. 121 and 122 with permission. Copyright 2021 John Wiley and Sons, and 2022 American Chemical Society, respectively.

discovered that a similar *in situ* polymerization process enables sPDA transfer to acrylate hydrogels (Fig. 9a),<sup>13</sup> with transfer dependent upon gel composition (Fig. 9b). The transferred PDA layer is also visible in cryoelectron microscopy, altering surface pore structure (Fig. 9c, main image) in comparison with unfunctionalized polyacrylamide (PAAm, Fig. 9c, inset). When amine PDA layers are transferred to the hydrogel surface, they

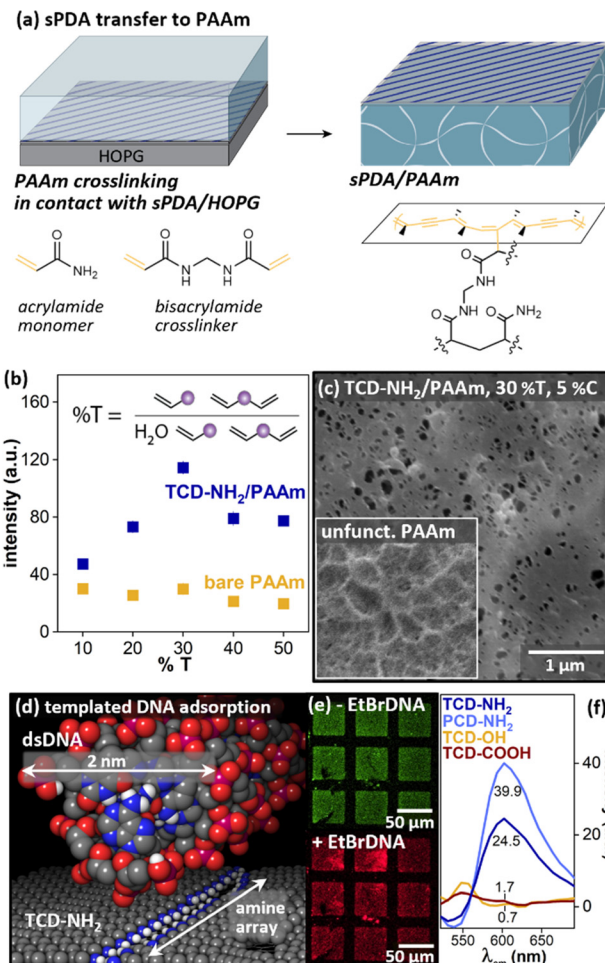


**Fig. 9** (a) Schematic of sPDA transfer from HOPG to PAAm. (b) sPDA fluorescence emission with varying PAAm composition. (c) Cryoelectron microscopy of functionalized and unfunctionalized PAAm, illustrating difference in pore structure. (d) Molecular model of dsDNA and TCD-NH<sub>2</sub>, illustrating relative size scales of functional patterns. (e) Microcontact patterned TCD-NH<sub>2</sub>/PAAm without (top) and with (bottom) exposure to EtBr-labeled dsDNA. (f) Fluorescence emission from amine, hydroxyl, and carboxylic-acid functionalized PAAm surfaces after exposure to EtBr-DNA, illustrating impact of amine functional group on dsDNA adsorption. Adapted from ref. 13 with permission. Copyright 2022 American Chemical Society.

template adsorption of charged electrolytes such as DNA (molecular model, Fig. 9d, experimental data, Fig. 9e and f). More broadly, these findings may point to utility of sPDA monolayers in structuring multivalent binding interactions with analytes in the environment.

## Outlook

While much of the work on high-resolution surface patterning to date has focused on hard, often crystalline, surfaces, there is a growing need for methods that enable scalable, high-resolution patterning of soft materials for interfaces with biology. A number of studies have illustrated that direct





translation of methods that are effective in patterning hard materials produce much larger feature sizes in soft materials.

We suggest that self-assembled molecular networks and other similar chemical patterning strategies represent a powerful and underutilized toolkit for high-resolution chemical control of soft interfaces. In particular, molecular networks that allow for on-surface reactivity enable patterns to be assembled on hard, crystalline materials, covalently locked, and then transferred to soft materials, as long as the polymerized pattern has total dimensions that exceed the scale of surface defects (e.g. pores) in the soft material. Here, we have focused on a class of chemical patterns based on polydiacetylenes, in which the polydiacetylene backbone itself acts as a structural integrity element, and as an optical readout of transfer. More broadly, given the resurgence of interest in on-surface reactions in relation to catalysis and other applications, there are likely to be a wide range of structural motifs that exhibit similar behavior.

We note that integration of high-resolution patterning strategies with soft materials creates a parallel need for high-resolution interfacial characterization strategies that work well at such material interfaces. Many high-resolution interfacial characterization methods to date depend on an intersection of material properties (e.g. conductivity) that exclude soft materials such as hydrogels. Techniques such as super-resolution optical microscopy that operate on soft materials typically require complex fluorescent labels, complicating interface design. Again, because on-surface molecular assembly and reaction pathways have often focused on materials that embed conjugated bond networks, for molecular electronics and other applications, there are likely to be many classes of materials that provide useful optical readouts of transfer.

## Author contributions

A. S., A. S. and S. A. C. wrote the manuscript. S. A. C. edited the manuscript.

## Conflicts of interest

There are no conflicts to declare.

## Acknowledgements

S. A. C. Acknowledges support through an NSF grant, NSF-CHE-MSN 2108966.

## Notes and references

- 1 Y. Q. Chen, Z. W. Shu, S. Zhang, P. Zeng, H. K. Liang, M. J. Zheng and H. G. Duan, Sub-10 nm Fabrication: Methods and Applications, *Int. J. Extreme Manuf.*, 2021, 3, 032002.
- 2 S. V. Graeter, J. H. Huang, N. Perschmann, M. Lopez-Garcia, H. Kessler, J. D. Ding and J. P. Spatz, Mimicking Cellular Environments by Nanostructured Soft Interfaces, *Nano Lett.*, 2007, 7, 1413–1418.
- 3 M. Kremer, E. Pothmann, T. Rossler, J. Baker, A. Yee, H. Blach and J. M. Prausnitz, Pore-Size Distributions of Cationic Polyacrylamide Hydrogels Varying in Initial Monomer Concentration and Cross-Linker/Monomer Ratio, *Macromolecules*, 1994, 27, 2965–2973.
- 4 N. Weiss and A. Silberberg, Inhomogeneity of Polyacrylamide Gel Structure from Permeability and Viscoelasticity, *Br. Polym. J.*, 1977, 9, 144–150.
- 5 N. Annabi, J. W. Nichol, X. Zhong, C. Ji, S. Koshy, A. Khademhosseini and F. Dehghani, Controlling the Porosity and Micro-architecture of Hydrogels for Tissue Engineering, *Tissue Eng., Part B*, 2010, 16, 371–383.
- 6 L. Capodieci, From Optical Proximity Correction to Lithography-Driven Physical Design (1996–2006): 10 Years of Resolution Enhancement Technology and the Roadmap Enablers for the Next Decade. Proc. SPIE: Opt. Microlithog. XIX 2006, 6154, 615401.
- 7 J. E. E. Baglin, Ion Beam Nanoscale Fabrication and Lithography—a Review, *Appl. Surf. Sci.*, 2012, 258, 4103–4111.
- 8 F. S. Bates, M. A. Hillmyer, T. P. Lodge, C. M. Bates, K. T. Delaney and G. H. Fredrickson, Multiblock Polymers: Panacea or Pandora's Box?, *Science*, 2012, 336, 434–440.
- 9 A. Kumar, H. A. Biebuyck and G. M. Whitesides, Patterning Self-Assembled Monolayers: Applications in Materials Science, *Langmuir*, 1994, 10, 1498–1511.
- 10 S. A. Claridge, W.-S. Liao, J. C. Thomas, Y. Zhao, H. H. Cao, S. Cheunkar, A. C. Serino, A. M. Andrews and P. S. Weiss, From the Bottom Up: Dimensional Control and Characterization in Molecular Monolayers, *Chem. Soc. Rev.*, 2013, 42, 2725–2745.
- 11 B. G. Munoz-Robles, I. Kopyeva and C. A. DeForest, Surface Patterning of Hydrogel Biomaterials to Probe and Direct Cell-Matrix Interactions, *Adv. Mater. Interfaces*, 2020, 7, 2001198.
- 12 T. C. Davis, J. O. Bechtold, A. Shi, E. N. Lang, A. Singh and S. A. Claridge, One Nanometer Wide Functional Patterns with a Sub-10 Nanometer Pitch Transferred to an Amorphous Elastomeric Material, *ACS Nano*, 2021, 15, 1426–1435.
- 13 J. C. Arango, L. O. Williams, A. Shi, A. Singh, E. K. Nava, R. V. Fisher, J. A. Garfield and S. A. Claridge, Nanostructured Surface Functionalization of Polyacrylamide Hydrogels Below the Length Scale of Hydrogel Heterogeneity, *ACS Appl. Mater. Interfaces*, 2022, 14(38), 43937–43945.
- 14 C. G. Willson, R. R. Dammel and A. Reiser, Photoresist Materials: A Historical Perspective, *Proc. SPIE: Adv. Resist Technol. Proc. XIV*, 1997, 3049, 275826.
- 15 G. J. Leggett, Photolithography Beyond the Diffraction Limit, in *Nanolithography and Patterning Techniques in Microelectronics*, D. Bucknell ed. Elsevier, 2005, pp. 238–266.
- 16 D. Fan and Y. Ekinci, Photolithography Reaches 6 nm Half-Pitch Using EUV Light, *Proc. SPIE*, 2016, 9776, 97761V.
- 17 V. Bakshi, *EUV Lithography*, SPIE Press, 2009.
- 18 J. Garofalo, C. J. Biddick, R. L. Kostelak and S. Vaidya, Mask Assisted Off-Axis Illumination Technique for Random Logic, *J. Vac. Sci. Technol., B*, 1993, 11, 2651–2658.
- 19 M. D. Levenson, N. S. Viswanathan and R. A. Simpson, Improving Resolution in Photolithography with a Phase-Shifting Mask, *IEEE Trans. Electron. Devices*, 1982, 29, 1828–1836.
- 20 V. R. Manfrinato, L. H. Zhang, D. Su, H. G. Duan, R. G. Hobbs, E. A. Stach and K. K. Berggren, Resolution Limits of Electron-Beam Lithography toward the Atomic Scale, *Nano Lett.*, 2013, 13, 1555–1558.
- 21 A. E. Grigorescu and C. W. Hagen, Resists for Sub-20 nm Electron Beam Lithography with a Focus on HSQ: State of the Art, *Nanotechnology*, 2009, 20, 292001.
- 22 A. A. Tseng, K. Chen, C. D. Chen and K. J. Ma, Electron Beam Lithography in Nanoscale Fabrication: Recent Developments, *IEEE Trans. Electron Devices*, 2003, 26, 141–149.
- 23 J. Orloff, Fundamental Limits to Imaging Resolution for Focused Ion Beams, *J. Vac. Sci. Technol., B: Microelectron. Nanometer Struct.–Process., Meas., Phenom.*, 1996, 14, 3759–3763.
- 24 K. Li, J. Li, C. Reardon, C. S. Schuster, Y. Wang, G. J. Triggs, N. Damnik, J. Muenchenberger, X. Wang, E. R. Martins and T. F. Krauss, High Speed E-Beam Writing for Large Area Photonic Nanostructures - a Choice of Parameters, *Sci. Rep.*, 2016, 6, 32945.
- 25 C. M. Bates, M. J. Maher, D. W. Janes, C. J. Ellison and C. G. Willson, Block Copolymer Lithography, *Macromolecules*, 2014, 47, 2–12.



- 26 W. J. Durand, G. Blachut, M. J. Maher, S. Sirard, S. Tein, M. C. Carlson, Y. Asano, S. X. Zhou, A. P. Lane, C. M. Bates, C. J. Ellison and C. G. Willson, Design of High-Chi Block Copolymers for Lithography, *J. Polym. Sci., Part A: Polym. Chem.*, 2015, **53**, 344–352.
- 27 C. M. Bates, T. Seshimo, M. J. Maher, W. J. Durand, J. D. Cushen, L. M. Dean, G. Blachut, C. J. Ellison and C. G. Willson, Polarity-Switching Top Coats Enable Orientation of Sub-10 nm Block Copolymer Domains, *Science*, 2012, **338**, 775–779.
- 28 J. G. Kennemur, L. Yao, F. S. Bates and M. A. Hillmyer, Sub-5 nm Domains in Ordered Poly(Cyclohexylethylene)-Block-Poly(Methyl Methacrylate) Block Polymers for Lithography, *Macromolecules*, 2014, **47**, 1411–1418.
- 29 G. G. Yang, H. J. Choi, K. H. Han, J. H. Kim, C. W. Lee, E. I. Jung, H. M. Jin and S. O. Kim, Block Copolymer Nanopatterning for Nonsemiconductor Device Applications, *ACS Appl. Mater. Interface*, 2022, **14**, 12011–12037.
- 30 M. Park, C. Harrison, P. M. Chaikin, R. A. Register and D. H. Adamson, Block Copolymer Lithography: Periodic Arrays of  $\sim 10^{11}$  Holes in 1 Square Centimeter, *Science*, 1997, **276**, 1401–1404.
- 31 M. P. Stoykovich, H. Kang, K. C. Daoulas, G. S. Liu, C. C. Liu, J. J. de Pablo, M. Muller and P. F. Nealey, Directed Self-Assembly of Block Copolymers for Nanolithography: Fabrication of Isolated Features and Essential Integrated Circuit Geometries, *ACS Nano*, 2007, **1**, 168–175.
- 32 B. Stel, I. Gunkel, X. Gu, T. P. Russell, J. J. De Yoreo and M. Lingenfelder, Contrasting Chemistry of Block Copolymer Films Controls the Dynamics of Protein Self-Assembly at the Nanoscale, *ACS Nano*, 2019, **13**, 4018–4027.
- 33 A. Kumar and G. M. Whitesides, Features of Gold Having Micrometer to Centimeter Dimensions Can Be Formed through a Combination of Stamping with an Elastomeric Stamp and an Alkanethiol Ink Followed by Chemical Etching, *Appl. Phys. Lett.*, 1993, **63**, 2002–2004.
- 34 A. Kumar, H. A. Biebuyck and G. M. Whitesides, Patterning Self-Assembled Monolayers – Applications in Materials Science, *Langmuir*, 1994, **10**, 1498–1511.
- 35 A. G. Castaño, V. Hortiguera, A. Lagunas, C. Cortina, N. Montserrat, J. Samitier and E. Martinez, Protein Patterning on Hydrogels by Direct Microcontact Printing: Application to Cardiac Differentiation, *RSC Adv.*, 2014, **4**, 29120–29123.
- 36 E. Delamar, H. Schmid, A. Bietsch, N. B. Larsen, H. Rothuizen, B. Michel and H. Biebuyck, Transport Mechanisms of Alkanethiols During Microcontact Printing on Gold, *J. Phys. Chem. B*, 1998, **102**, 3324–3334.
- 37 H.-W. Li, B. V. O. Muir, G. Fichet and W. T. S. Huck, Nanocontact Printing: A Route to Sub-50 nm-Scale Chemical and Biological Patterning, *Langmuir*, 2003, **19**, 1963–1965.
- 38 W. S. Liao, S. Cheunkar, H. H. Cao, H. R. Bednar, P. S. Weiss and A. M. Andrews, Subtractive Patterning Via Chemical Lift-Off Lithography, *Science*, 2012, **337**, 1517–1521.
- 39 C. Y. Chen, C. M. Wang and W. S. Liao, A Special Connection between Nanofabrication and Analytical Devices: Chemical Lift-Off Lithography, *Bull. Chem. Soc. Jpn.*, 2019, **92**, 600–607.
- 40 C. Y. Chen, C. M. Wang, H. H. Li, H. H. Chan and W. S. Liao, Wafer-Scale Bioactive Substrate Patterning by Chemical Lift-Off Lithography, *Beilstein J. Nanotechnol.*, 2018, **9**, 311–320.
- 41 S. Y. Chou, P. R. Krauss and P. J. Renstrom, Imprint Lithography with 25-Nanometer Resolution, *Science*, 1996, **272**, 85–87.
- 42 G. Y. Liu, S. Xu and Y. L. Qian, Nanofabrication of Self-Assembled Monolayers Using Scanning Probe Lithography, *Acc. Chem. Res.*, 2000, **33**, 457–466.
- 43 R. Garcia, A. W. Knoll and E. Riedo, Advanced Scanning Probe Lithography, *Nat. Nanotechnol.*, 2014, **9**, 577–587.
- 44 G. Q. Liu, S. H. Petrosko, Z. J. Zheng and C. A. Mirkin, Evolution of Dip-Pen Nanolithography (DPN): From Molecular Patterning to Materials Discovery, *Chem. Rev.*, 2020, **120**, 6009–6047.
- 45 R. D. Piner, J. Zhu, F. Xu, S. H. Hong and C. A. Mirkin, “Dip-Pen” Nanolithography, *Science*, 1999, **283**, 661–663.
- 46 A. Urtizberea, M. Hirtz and H. Fuchs, Ink Transport Modelling in Dip-Pen Nanolithography and Polymer Pen Lithography, *Nanofabrication*, 2016, **2**, 43–53.
- 47 K. A. Brown, D. J. Eichelsdoerfer, X. Liao, S. He and C. A. Mirkin, Material Transport in Dip-Pen Nanolithography, *Front. Phys.*, 2014, **9**, 385–397.
- 48 J. Jang, G. C. Schatz and M. A. Ratner, Capillary Force on a Nanoscale Tip in Dip-Pen Nanolithography, *Phys. Rev. Lett.*, 2003, **90**, 156104.
- 49 A. B. Braunschweig, F. Huo and C. A. Mirkin, Molecular Printing, *Nat. Chem.*, 2009, **1**, 353–358.
- 50 K. Salaita, Y. Wang, J. Fragala, R. A. Vega, C. Liu and C. A. Mirkin, Massively Parallel Dip-Pen Nanolithography with 55000-Pen Two-Dimensional Arrays, *Angew. Chem.*, 2006, **45**, 7220–7223.
- 51 F. Huo, Z. Zheng, G. Zheng, L. R. Giam, H. Zhang and C. A. Mirkin, Polymer Pen Lithography, *Science*, 2008, **321**, 1658–1660.
- 52 E. P. Chan and A. J. Crosby, Spontaneous Formation of Stable Aligned Wrinkling Patterns, *Soft Matter*, 2006, **2**, 324–328.
- 53 N. Bowden, S. Brittain, A. G. Evans, J. W. Hutchinson and G. M. Whitesides, Spontaneous Formation of Ordered Structures in Thin Films of Metals Supported on an Elastomeric Polymer, *Nature*, 1998, **393**, 146–149.
- 54 C. M. Kolodziej and H. D. Maynard, Electron-Beam Lithography for Patterning Biomolecules at the Micron and Nanometer Scale, *Chem. Mater.*, 2011, **24**, 774–780.
- 55 K. L. Christman, E. Schopf, R. M. Broyer, R. C. Li, Y. Chen and H. D. Maynard, Positioning Multiple Proteins at the Nanoscale with Electron Beam Cross-Linked Functional Polymers, *J. Am. Chem. Soc.*, 2009, **131**, 521–527.
- 56 V. R. Tirumala, R. Divan, L. E. Ocola and D. C. Mancini, Direct-Write E-Beam Patterning of Stimuli-Responsive Hydrogel Nanostructures, *J. Vac. Sci. Technol., B: Microelectron. Nanometer Struct.–Process., Meas., Phenom.*, 2005, **23**, 3124.
- 57 M. S. Hahn, J. S. Miller and J. L. West, Best, Laser Scanning Lithography for Surface Micropatterning on Hydrogels, *Adv. Mater.*, 2005, **17**, 2939–2942.
- 58 M. S. Hahn, J. S. Miller and J. L. West, Three-Dimensional Biochemical and Biomechanical Patterning of Hydrogels for Guiding Cell Behavior, *Adv. Mater.*, 2006, **18**, 2679–2684.
- 59 M. S. Hahn, L. J. Taite, J. J. Moon, M. C. Rowland, K. A. Ruffino and J. L. West, Photolithographic Patterning of Polyethylene Glycol Hydrogels, *Biomaterials*, 2006, **27**, 2519–2524.
- 60 I. Batalov, K. R. Stevens and C. A. DeForest, Photopatterned Biomolecule Immobilization to Guide Three-Dimensional Cell Fate in Natural Protein-Based Hydrogels, *Proc. Natl. Acad. Sci. U. S. A.*, 2021, **118**, e2014194118.
- 61 C. A. DeForest, B. D. Polizzotti and K. S. Anseth, Sequential Click Reactions for Synthesizing and Patterning Three-Dimensional Cell Microenvironments, *Nat. Mater.*, 2009, **8**, 659–664.
- 62 C. A. DeForest and K. S. Anseth, Cytocompatible Click-Based Hydrogels with Dynamically Tunable Properties through Orthogonal Photoconjugation and Photocleavage Reactions, *Nat. Chem.*, 2011, **3**, 925–931.
- 63 C. A. DeForest, E. A. Sims and K. S. Anseth, Peptide-Functionalized Click Hydrogels with Independently Tunable Mechanics and Chemical Functionality for 3D Cell Culture, *Chem. Mater.*, 2010, **22**, 4783–4790.
- 64 F. Guilak, D. M. Cohen, B. T. Estes, J. M. Gimble, W. Liedtke and C. S. Chen, Control of Stem Cell Fate by Physical Interactions with the Extracellular Matrix, *Cell Stem Cell*, 2009, **5**, 17–26.
- 65 S. Raghavan and C. S. Chen, Micropatterned Environments in Cell Biology, *Adv. Mater.*, 2004, **16**, 1303–1313.
- 66 R. McBeath, D. M. Pirone, C. M. Nelson, K. Bhadriraju and C. S. Chen, Cell Shape, Cytoskeletal Tension, and RhoA Regulate Stem Cell Lineage Commitment, *Dev. Cell*, 2004, **6**, 483–495.
- 67 M. R. Burnham, J. N. Turner, D. Szarowski and D. L. Martin, Biological Functionalization and Surface Micropatterning of Polyacrylamide Hydrogels, *Biomaterials*, 2006, **27**, 5883–5891.
- 68 D. P. Goronzy, M. Ebrahimi, F. Rosei, Arramel, Y. Fang, S. De Feyter, S. L. Tait, C. Wang, P. H. Beton, A. T. S. Wee, P. S. Weiss and D. F. Perepichka, Supramolecular Assemblies on Surfaces: Nanopatterning, Functionality, and Reactivity, *ACS Nano*, 2018, **12**, 7445–7481.
- 69 A. Shi and S. A. Claridge, Lipids: An Atomic Toolkit for the Endless Frontier, *ACS Nano*, 2021, **15**, 15429–15445.
- 70 A. J. Groszek, Preferential Adsorption of Normal Hydrocarbons on Cast Iron, *Nature*, 1962, **196**, 531–533.
- 71 A. J. Groszek, Preferential Adsorption of Long-Chain Normal Paraffins on MoS<sub>2</sub>, WS<sub>2</sub> and Graphite from N-Heptane, *Nature*, 1964, **204**, 680.





- 72 A. J. Groszek, Selective Adsorption at Graphite/Hydrocarbon Interfaces, *Proc. R. Soc. London, Ser. A*, 1970, **314**, 473.
- 73 J. P. Rabe and S. Buchholz, Commensurability and Mobility in 2-Dimensional Molecular Patterns on Graphite, *Science*, 1991, **253**, 424–427.
- 74 D. M. Cyr, B. Venkataraman and G. W. Flynn, STM Investigations of Organic Molecules Physisorbed at the Liquid-Solid Interface, *Chem. Mater.*, 1996, **8**, 1600–1615.
- 75 D. M. Cyr, B. Venkataraman, G. W. Flynn, A. Black and G. M. Whitesides, Functional Group Identification in Scanning Tunneling Microscopy of Molecular Adsorbates, *J. Phys. Chem.*, 1996, **100**, 13747–13759.
- 76 S. De Feyter and F. C. De Schryver, Self-Assembly at the Liquid/Solid Interface: STM Reveals, *J. Phys. Chem. B*, 2005, **109**, 4290–4302.
- 77 J. M. MacLeod and F. Rosei, Molecular Self-Assembly on Graphene, *Small*, 2014, **10**, 1038–1049.
- 78 J. A. Mann and W. R. Dichtel, Noncovalent Functionalization of Graphene by Molecular and Polymeric Adsorbates, *J. Phys. Chem. Lett.*, 2013, **4**, 2649–2657.
- 79 S. Furukawa, H. Uji-i, K. Tahara, T. Ichikawa, M. Sonoda, F. C. De Schryver, Y. Tobe and S. De Feyter, Molecular Geometry Directed Kagome and Honeycomb Networks: Toward Two-Dimensional Crystal Engineering, *J. Am. Chem. Soc.*, 2006, **128**, 3502–3503.
- 80 K. Tahara, S. Furukawa, H. Uji-i, T. Uchino, T. Ichikawa, J. Zhang, W. Mamdouh, M. Sonoda, F. C. De Schryver, S. De Feyter and Y. Tobe, Two-Dimensional Porous Molecular Networks of Dehydrobenzo[12]Annulene Derivatives Via Alkyl Chain Interdigitation, *J. Am. Chem. Soc.*, 2006, **128**, 16613–16625.
- 81 J. Liu, T. Chen, X. Deng, D. Wang, J. Pei and L.-J. Wan, Chiral Hierarchical Molecular Nanostructures on Two-Dimensional Surface by Controllable Trinary Self-Assembly, *J. Am. Chem. Soc.*, 2011, **133**, 21010–21015.
- 82 R. Gutzler, C. Fu, A. Dadvand, Y. Hua, J. M. MacLeod, F. Rosei and D. F. Perepichka, Halogen Bonds in 2D Supramolecular Self-Assembly of Organic Semiconductors, *Nanoscale*, 2012, **4**, 5965–5971.
- 83 Q.-N. Zheng, X.-H. Liu, T. Chen, H.-J. Yan, T. Cook, D. Wang, P. J. Stang and L.-J. Wan, Formation of Halogen Bond-Based 2D Supramolecular Assemblies by Electric Manipulation, *J. Am. Chem. Soc.*, 2015, **137**, 6128–6131.
- 84 Y. H. Wei, W. J. Tong and M. B. Zimmt, Self-Assembly of Patterned Monolayers with Nanometer Features: Molecular Selection Based on Dipole Interactions and Chain Length, *J. Am. Chem. Soc.*, 2008, **130**, 3399–3405.
- 85 Y. Wei, W. J. Tong, C. Wise, X. D. Wei, K. Armbrust and M. B. Zimmt, Dipolar Control of Monolayer Morphology: Spontaneous SAM Patterning, *J. Am. Chem. Soc.*, 2006, **128**, 13362–13363.
- 86 P. C. M. Grim, S. De Feyter, A. Gesquiere, P. Vanoppen, M. Rucker, S. Valiyaveetil, G. Moessner, K. Mullen and F. C. De Schryver, Submolecularly Resolved Polymerization of Diacetylene Molecules on the Graphite Surface Observed with Scanning Tunneling Microscopy, *Angew. Chem., Int. Ed.*, 1997, **36**, 2601–2603.
- 87 M. Akai-Kasaya, K. Shimizu, Y. Watanabe, A. Saito, M. Aono and Y. Kuwahara, Electronic Structure of a Polydiacetylene Nanowire Fabricated on Highly Ordered Pyrolytic Graphite, *Phys. Rev. Lett.*, 2003, **91**, 255501.
- 88 G. S. McCarty and P. S. Weiss, Formation and Manipulation of Protopolymer Chains, *J. Am. Chem. Soc.*, 2004, **126**, 16772–16776.
- 89 J. A. Lipton-Duffin, O. Ivasenko, D. F. Perepichka and F. Rosei, Synthesis of Polyphenylene Molecular Wires by Surface-Confined Polymerization, *Small*, 2009, **5**, 592–597.
- 90 M. M. Blake, S. U. Nanayakkara, S. A. Claridge, L. C. Fernandez-Torres, E. C. H. Sykes and P. S. Weiss, Identifying Reactive Intermediates in the Ullmann Coupling Reaction by Scanning Tunneling Microscopy and Spectroscopy, *J. Phys. Chem. A*, 2009, **113**, 13167–13172.
- 91 J. W. Colson and W. R. Dichtel, Rationally Synthesized Two-Dimensional Polymers, *Nat. Chem.*, 2013, **5**, 453–465.
- 92 N. A. A. Zwaneveld, R. Pawlak, M. Abel, D. Catalin, D. Gimes, D. Bertin and L. Porte, Organized Formation of 2D Extended Covalent Organic Frameworks at Surfaces, *J. Am. Chem. Soc.*, 2008, **130**, 6678–6679.
- 93 S. Spitzer, A. Rastgoo-Lahrood, K. Macknapp, V. Ritter, S. Sotier, W. M. Heckl and M. Lackinger, Solvent-Free on-Surface Synthesis of Boroxine COF Monolayers, *Chem. Commun.*, 2017, **53**, 5147–5150.
- 94 J. W. Colson, A. R. Woll, A. Mukherjee, M. P. Levendorf, E. L. Spitzer, V. B. Shields, M. G. Spencer, J. Park and W. R. Dichtel, Oriented 2D Covalent Organic Framework Thin Films on Single-Layer Graphene, *Science*, 2011, **332**, 228–231.
- 95 C. Bubeck, B. Tiede and G. Wegner, Sensitization of the Photopolymerization of Diacetylenes Studied in Multilayers, *Ber. Bunsenges.*, 1982, **86**, 495–498.
- 96 G. Wegner, Topochemical Reactions of Monomers with Conjugated Triple Bonds. I. Polymerization of 2,4-Hexadiyn-1,6-Diols Derivatives in Crystalline State, *Z. Naturforsch., B: J. Chem. Sci.*, 1969, **B 24**, 824–826.
- 97 G. Wegner, Topochemical Reactions of Monomers with Conjugated Triple Bonds. 3. Solid-State Reactivity of Derivatives of Diphenyldiacetylene, *J. Polym. Sci., Part B: Polym. Lett.*, 1971, **9**, 133–144.
- 98 G. Wegner, Topochemical Polymerization of Monomers with Conjugated Triple Bonds, *Makromol. Chem.*, 1972, **154**, 35–48.
- 99 B. Tiede, G. Wegner, D. Naegele and H. Ringsdorf, Polymerization of Tricoso-10,12-Diynoic Acid in Multilayers, *Angew. Chem., Int. Ed. Engl.*, 1976, **15**, 764–765.
- 100 G. Lieser, B. Tiede and G. Wegner, Structure, Phase-Transitions and Polymerizability of Multilayers of Some Diacetylene Monocarboxylic Acids, *Thin Solid Films*, 1980, **68**, 77–90.
- 101 Y. Okawa and M. Aono, Materials Science - Nanoscale Control of Chain Polymerization, *Nature*, 2001, **409**, 683–684.
- 102 Y. Okawa and M. Aono, Linear Chain Polymerization Initiated by a Scanning Tunneling Microscope Tip at Designated Positions, *J. Chem. Phys.*, 2001, **115**, 2317–2322.
- 103 S. K. Mandal, Y. Okawa, T. Hasegawa and M. Aono, Rate-Determining Factors in the Chain Polymerization of Molecules Initiated by Local Single-Molecule Excitation, *ACS Nano*, 2011, **5**, 2779–2786.
- 104 Y. Okawa, M. Akai-Kasaya, Y. Kuwahara, S. K. Mandal and M. Aono, Controlled Chain Polymerisation and Chemical Soldering for Single-Molecule Electronics, *Nanoscale*, 2012, **4**, 3013–3028.
- 105 J. J. Bang, K. K. Rupp, S. R. Russell, S. W. Choong and S. A. Claridge, Sitting Phases of Polymerizable Amphiphiles for Controlled Functionalization of Layered Materials, *J. Am. Chem. Soc.*, 2016, **138**, 4448–4457.
- 106 T. A. Villarreal, S. R. Russell, J. J. Bang, J. K. Patterson and S. A. Claridge, Modulating Wettability of Layered Materials by Controlling Ligand Polar Headgroup Dynamics, *J. Am. Chem. Soc.*, 2017, **139**, 11973–11979.
- 107 S. W. Choong, S. R. Russell, J. J. Bang, J. K. Patterson and S. A. Claridge, Sitting Phase Monolayers of Polymerizable Phospholipids Create Dimensional, Molecular-Scale Wetting Control for Scalable Solution Based Patterning of Layered Materials, *ACS Appl. Mater. Interface*, 2017, **9**, 19326–19334.
- 108 T. R. Hayes, J. J. Bang, T. C. Davis, C. F. Peterson, D. G. McMillan and S. A. Claridge, Multimicrometer Noncovalent Monolayer Domains on Layered Materials through Thermally Controlled Langmuir-Schaefer Conversion for Noncovalent 2D Functionalization, *ACS Appl. Mater. Interface*, 2017, **9**, 36409–36416.
- 109 J. J. Bang, A. G. Porter, T. C. Davis, T. R. Hayes and S. A. Claridge, Spatially Controlled Noncovalent Functionalization of 2D Materials Based on Molecular Architecture, *Langmuir*, 2018, **34**, 5454–5463.
- 110 T. C. Davis, J. J. Bang, J. T. Brooks, D. G. McMillan and S. A. Claridge, Hierarchical Noncovalent Functionalization of 2D Materials by Controlled Langmuir-Schaefer Conversion, *Langmuir*, 2018, **34**, 1353–1362.
- 111 T. R. Hayes, E. N. Lang, A. Shi and S. A. Claridge, Large-Scale Noncovalent Functionalization of 2D Materials through Thermally Controlled Rotary Langmuir-Schaefer Conversion, *Langmuir*, 2020, **36**, 10577–10586.
- 112 T. C. Davis, J. O. Bechtold, T. R. Hayes, T. A. Villarreal and S. A. Claridge, Hierarchically Patterned Striped Phases of Phospholipids: Toward Controlled Presentation of Carbohydrates, *Faraday Discuss.*, 2019, **219**, 229–243.
- 113 S. R. Russell, T. C. Davis, M. G. Clark, T. R. Hayes and S. A. Claridge, Displaceable Templates with Sub-10 nm Periodicity Activate and Direct Epitaxial Assembly of Complex Aromatic Molecules, *Chem. Mater.*, 2020, **32**, 2552–2560.



- 114 M. A. Mezour, I. I. Perepichka, J. Zhu, R. B. Lennox and D. F. Perepichka, Directing the Assembly of Gold Nanoparticles with Two-Dimensional Molecular Networks, *ACS Nano*, 2014, **8**, 2214–2222.
- 115 S. Hoepfner, L. F. Chi and H. Fuchs, Formation of Au-55 Strands on a Molecular Template at the Solid–Liquid Interface, *Nano Lett.*, 2002, **2**, 459–463.
- 116 A. G. Porter, T. Ouyang, T. R. Hayes, J. Biechele-Speziale, S. R. Russell and S. A. Claridge, 1 nm-Wide Hydrated Dipole Arrays Regulate AuNW Assembly on Striped Monolayers in Nonpolar Solvent, *Chem*, 2019, **5**, 2264–2275.
- 117 E. N. Lang, A. G. Porter, T. Ouyang, A. Shi, T. R. Hayes, T. C. Davis and S. A. Claridge, Oleylamine Impurities Regulate Temperature-Dependent Hierarchical Assembly of Ultranarrow Gold Nanowires on Biotemplated Interfaces, *ACS Nano*, 2021, **15**, 10275–10285.
- 118 E. N. Lang, C. Pintro and S. A. Claridge, Trans and Saturated Alkyl Impurities in Technical-Grade Oleylamine: Limited Miscibility and Impacts on Nanocrystal Growth, *Chem. Mater.*, 2022, **34**, 5273–5282.
- 119 E. N. Lang and S. A. Claridge, Cow-to-Cow Variation in Nanocrystal Synthesis: Learning from Technical-Grade Oleylamine, *Nanotechnology*, 2022, **33**, 082501.
- 120 J. O. Bechtold, J. C. Arango, A. Shi, A. Singh and S. A. Claridge, Striped Poly(Diacetylene) Monolayers Control Adsorption of Polyelectrolytes and Proteins on 2D Materials and Elastomers, *ACS Appl. Nano Mater.*, 2021, **4**, 7037–7046.
- 121 A. Shi, T. A. Villarreal, A. Singh, T. R. Hayes, T. C. Davis, J. T. Brooks and S. A. Claridge, Plenty of Room at the Top: A Multi-Scale Understanding of nm-Resolution Polymer Patterning on 2D Materials, *Angew. Chem., Int. Ed.*, 2021, **60**, 25436–25444.
- 122 A. Shi, A. Singh, L. O. Williams, J. C. Arango and S. A. Claridge, Nanometer-Scale Precision Polymer Patterning of PDMS: Multi-scale Insights into Patterning Efficiency Using Alkylidynamines, *ACS Appl. Mater. Interfaces*, 2022, **14**, 22634–22642.

